Electronic Supplementary Material (ESI) for ChemComm.

Supplementary Information

Rotation of a helical coordination polymer by mechanical grinding

Bibhuti Bhusan Rath,[a] Goutam Kumar Kole,[b] Samuel Alexander Morris,*[,c] Jagadese J. Vittal*[,a]

[a] Department of Chemistry, National University of Singapore, SINGAPORE 117543 E-mail: chmjjv@nus.edu.sg; Fax: +65-6779-1691

[b] Department of Chemistry and Research Institute, SRM Institute of Science and Technology, Kattankulathur, Tamil Nadu 603203, India

[c] School of Materials Science and Engineering, Nanyang Technological University, 50 Nanyang Avenue, SINGAPORE 639798. E-mail: smorris@ntu.edu.sg

Materials and General Methods

All solvents and reagents were commercially available and used as received without further purification. *Trans*-5-Styrylpyrimidine (5-Spym) ligand was synthesized by performing Heck coupling reaction according to previously reported literature.[1]

Bruker D8 Venture Single Crystal X-ray Diffractometer (SCXRD) was used for collecting intensity data of single crystals. Powder X-ray diffraction (PXRD) analysis were performed on a D5005 Siemens X-ray diffractometer with graphite monochromatized CuK_α radiation (λ = 1.54056) at RT (298 K). ^{1}H NMR spectra were recorded on a 400 MHz Bruker Avance 400 FT NMR spectrometer with TMS as an internal reference in DMSO-d_6 solution. $^{31}P\{^1H\}$ NMR spectra were recorded on a Bruker Avance spectrometer operating at 161.92 MHz with 85% H_3PO_4 as external reference. Solid state absorbance UV-vis spectra were measured on UV-2450 Shimadzu UV-visible spectrometer equipped with an integrating sphere and barium sulphate as reference. The solid-state photoluminescence measurements were made using Horiba Fluorolog with a solid-state sample holder. Thermogravimetric analysis (TGA) was performed under nitrogen atmosphere with a heating rate of 5°C min^{-1} on a TA instruments SDT-2960. The FT-IR spectra were recorded using Varian Excalibur 3100 spectrometer with KBr pellets. JEOL JSM-6701F Field Emission Scanning Electron Microscope (FESEM) was used for SEM images. JEOL JEM-3011 Transmission Electron Microscope installed with a LaB6 emitter and a Gatan Orius SC200 CCD camera was used for HRTEM images.The elemental analyses (C, H, N) were carried out by using ElementarVario Micro Cube instrument at the Elemental Analysis Lab, CMMAC, Department of Chemistry, National University of Singapore.

Solid state UV experiments

LUZCHEM UV reactor (wavelength 360 nm) was used for all UV-irradiation experiments. Crystalline ground powder was packed between the glass slides and irradiated under UV light. In order to maintain uniform exposure of UV radiation glass slides were flipped at regular intervals of time. Samples were taken out at regular intervals of time, dissolved in DMSO-d_6 for ^{1}H NMR experiments.

Preparation of [(Ph_3P)Ag(5-Spym)(OTf)]·0.75MeOH, 1: Compound **1** was prepared by reacting AgOTf (12.8 mg, 0.05 mmol), 5-Spym (9.1 mg, 0.05 mmol) and PPh_3 (13.1 mg, 0.05 mmol) in methanol at room temperature for 1 h. Diffraction quality colourless block shaped single crystals were obtained within few days by slow evaporation of the reaction mixture, which were filtered and air dried. Yield (53%). Elemental analysis for **1** (%) Calculated: C 52.56, H 3.89, N 3.86; Found: C 53.18, H 3.50, N 4.16; FT-IR (KBr pellet, cm^{-1}): 3455, 3053, 1889, 1638, 1575, 1480, 1436, 1284, 1158, 1098, 965, 915, 846, 749, 694, 637, 574, 520, 499, 439; ^{1}H NMR (400 MHz, 298 K, d_6-DMSO):): δ_H = 9.05 (m, 3H, pym-H of 5-Spym), 7.64 (m, 2H, Ph-H of 5-Spym), 7.56 (m, 9H, Ph-H of PPh_3), 7.55 (d, 1H, HC=CH of 5-Spym), 7.46 (m, 6H, Ph-H of

PPh_3), 7.43 (m, 2H, Ph-H of 5-Spym), 7.34 (t, 1H, Ph-H of 5-Spym), 7.26 (d, 1H, HC=CH of 5-Spym); ^{31}P NMR (161.92 MHz, 298K, $CDCl_3$): δ_P = 12.15

Crystal data for **1** at 100(2) K (CCDC **1989895**): $C_{31.75}H_{28}AgF_3N_2O_{3.75}PS$, M= 725.46; Monoclinic, $P2_1/n$; a = 26.6378(6), b = 9.0287(2), c = 27.6480(6) Å; α = 90, β = 110.8540(10), γ = 90°; V = 6213.9(2) Å^3; Z = 8; ρ_{calc} = 1.551 g.cm^{-3}; μ = 0.824 mm^{-1}; GOF = 1.058; final R_1 = 0.0517; wR_2 = 0.1089 [for 11314 data $I > 2\sigma(I)$].

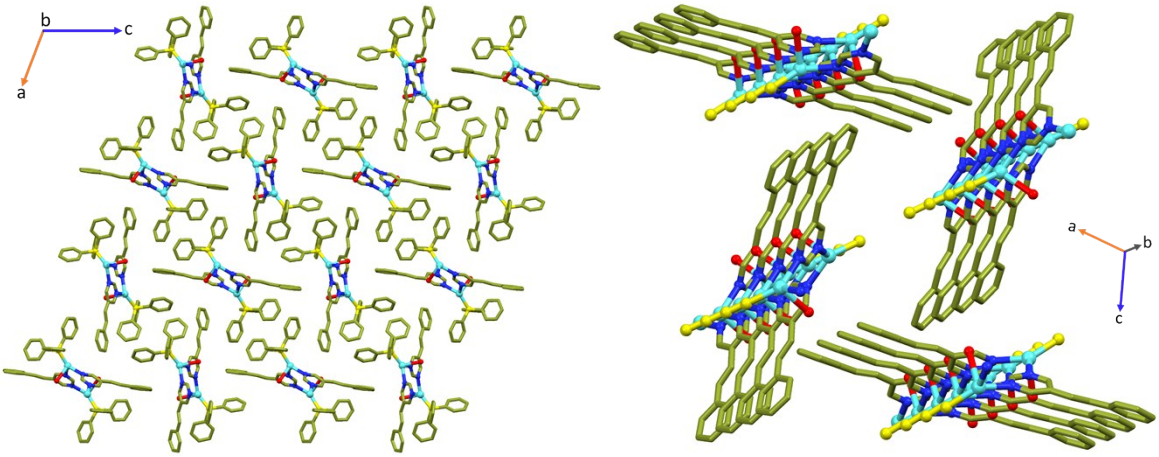

(a) (b)

Fig. S1 (a) A view of **1** along *b*-axis showing the helical chains and the relative alignments of the 5-Spym ligands and PPh_3 ligands (b) Another orientation of **1** shows the propagation of helical chain along *b*-axis and the relative orthogonal orientation of the 5-Spym ligands. Anions, hydrogen atoms and guest solvents are omitted for clarity.

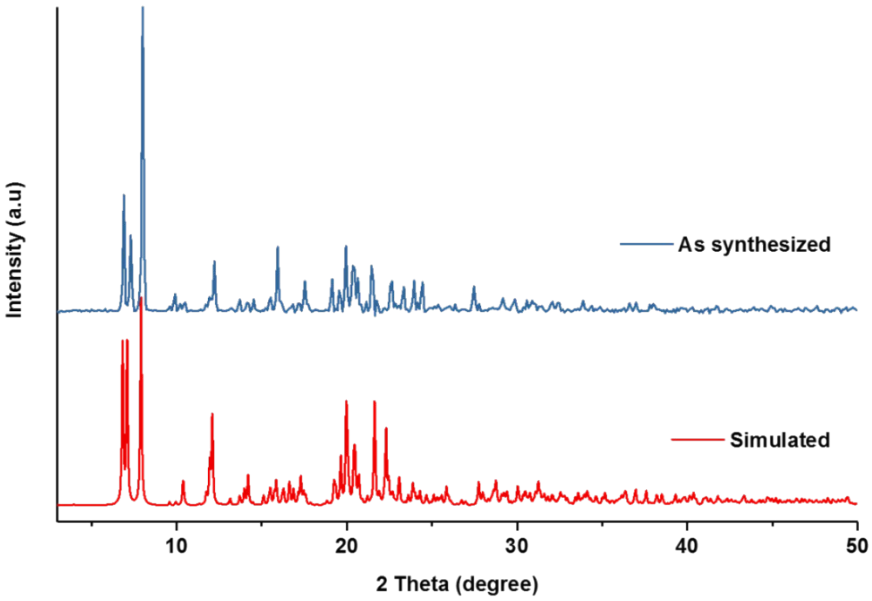

Fig. S2 Comparison of simulated and experimental PXRD patterns of compound **1**.

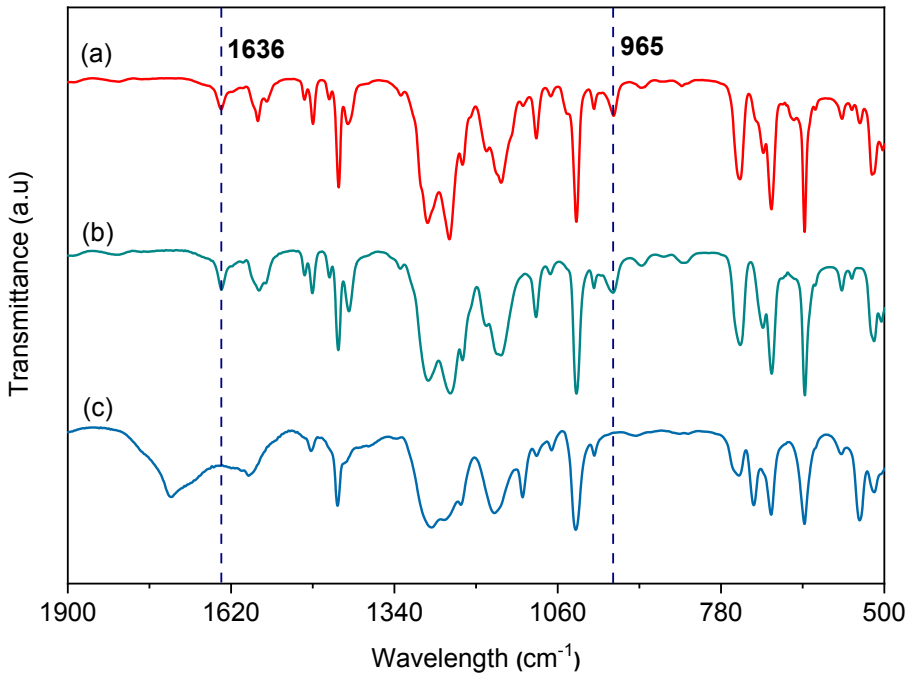

Fig. S3 FT-IR spectra of (a) crystal of compound **1**, (b) compound **1** after 30 min grinding, (c) 30 min ground sample after dimerization. Disappearance of the C=C stretching at 1636 cm^{-1} and =C-H out of plane bending at 965 cm^{-1} suggest the conversion of the olefinic group to cyclobutane group, thus confirming the photodimerization.

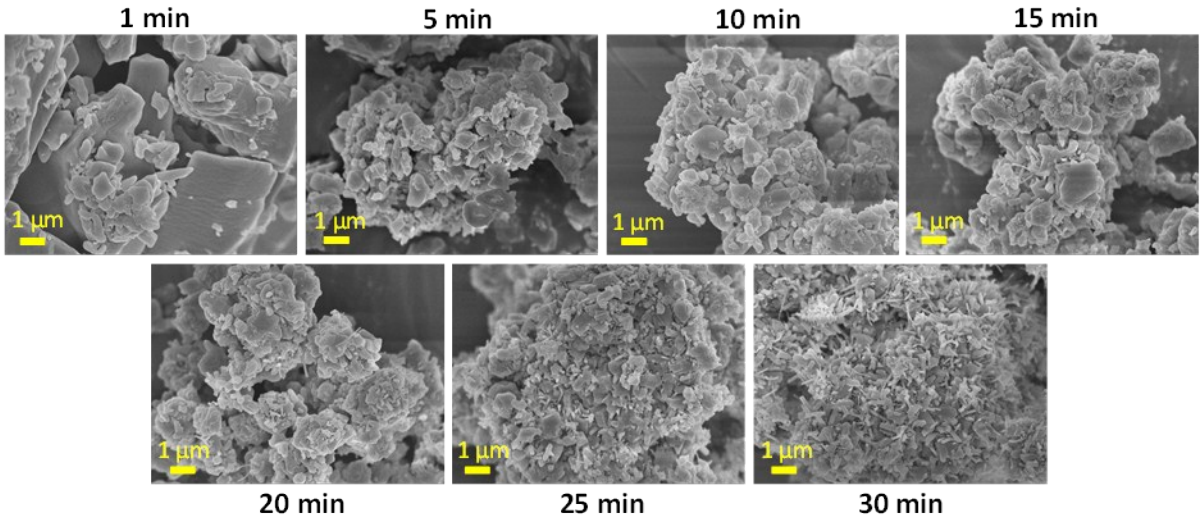

Fig. S4 SEM images of compound **1** in different grinding time. Particle size decreases gradually with grinding, ultimately forming plate like particles after 30 min grinding. (magnification ×10000)

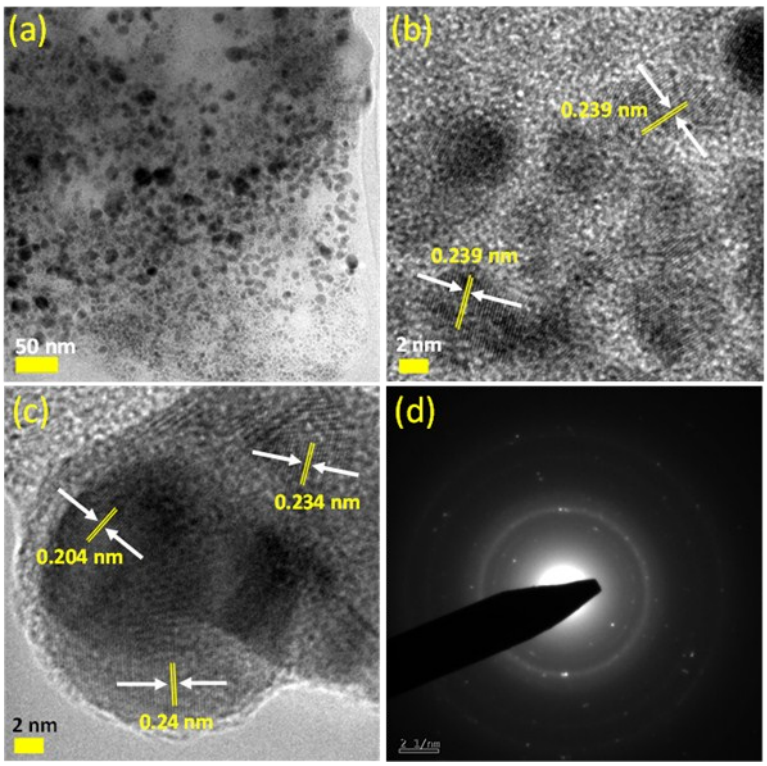

Fig. S5 HRTEM images of compound **1** after grinding time 30 min. (a) Shows crystalline particles at nanometer scale, (b) higher magnification clearly shows lattice fringes and calculated *d*-spacing, (c) A selected area shows lattice fringes of different orientation and calculated *d*-spacings and (d) SEAD pattern of the previous image clearly shows crystalline nature of the sample.

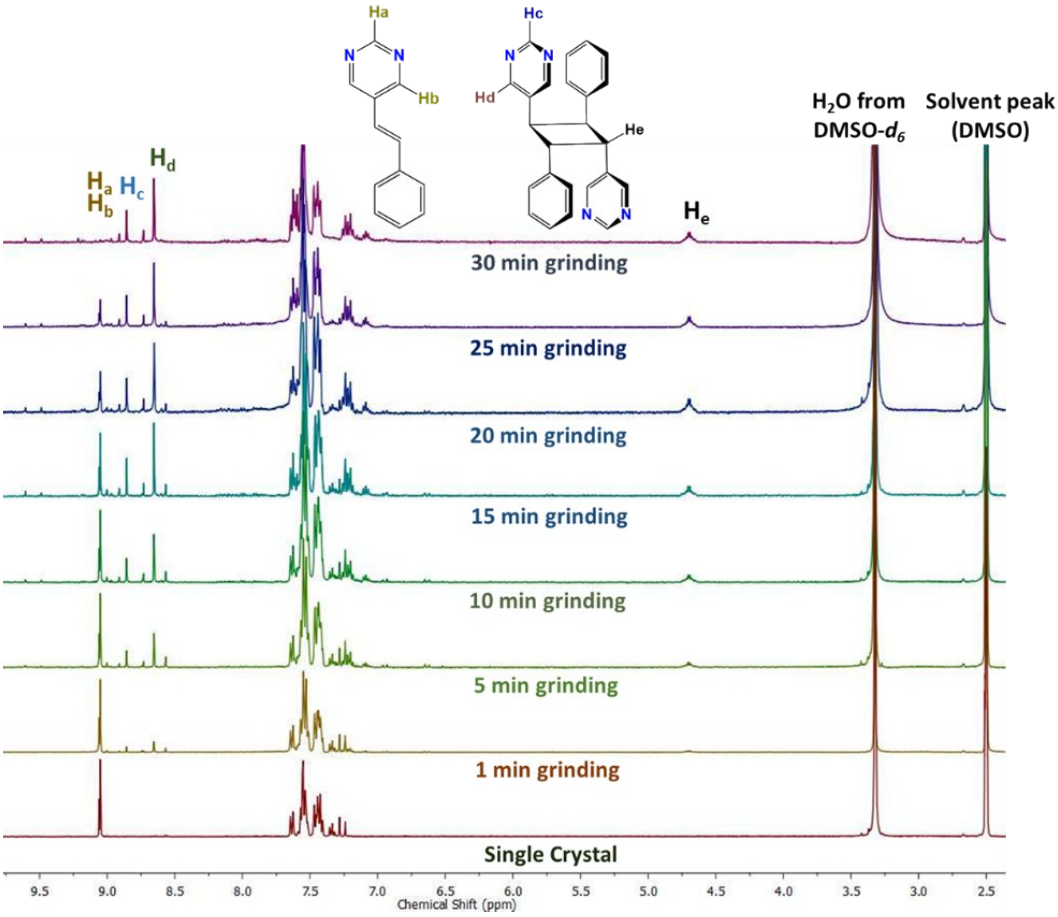

Fig. S6 ^{1}H-NMR spectra of **1** (single crystal and ground sample) in DMSO-d_6 subjected to UV irradiation. All the samples were irradiated for 72h while 30 min grinding sample was irradiated for 25h. The percentage of photodimerization was calculated by considering ^{1}H NMR peaks for H_a, H_b and H_c, H_d and other unidentified peaks. The peaks for H_a, H_b which appear as single peak for 5-Spym ligand, gradually split into two distinct peaks (assigned for H_c and H_d of the *Head-to-Tail* dimer) upon UV irradiation. In case of 30 min ground sample, complete disappearance of H_a, H_b indicates 100% conversion of 5-Spym ligand. However, 83% dimerized product formed along with some unidentified products.

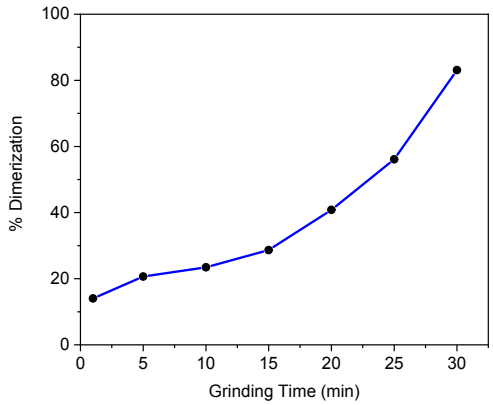

Fig. S7 Correlation between % dimerization and grinding time. Sample for 30 min grinding was exposed to UV irradiation for 25h while all other samples were exposed for 72h.

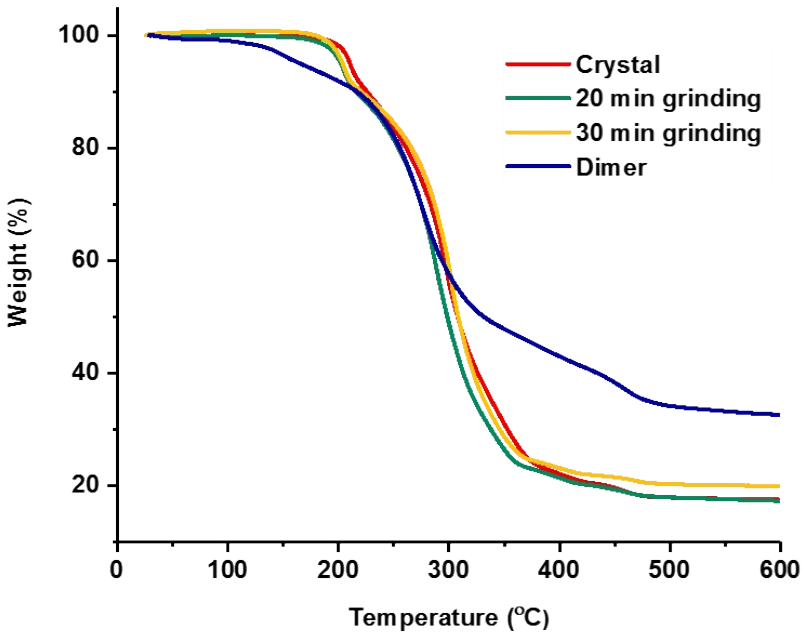

Fig. S8 TGA curves for different samples of compound **1**. No solvent loss was observed in case of crystal as solvent might have lost from the lattice at room temperature.

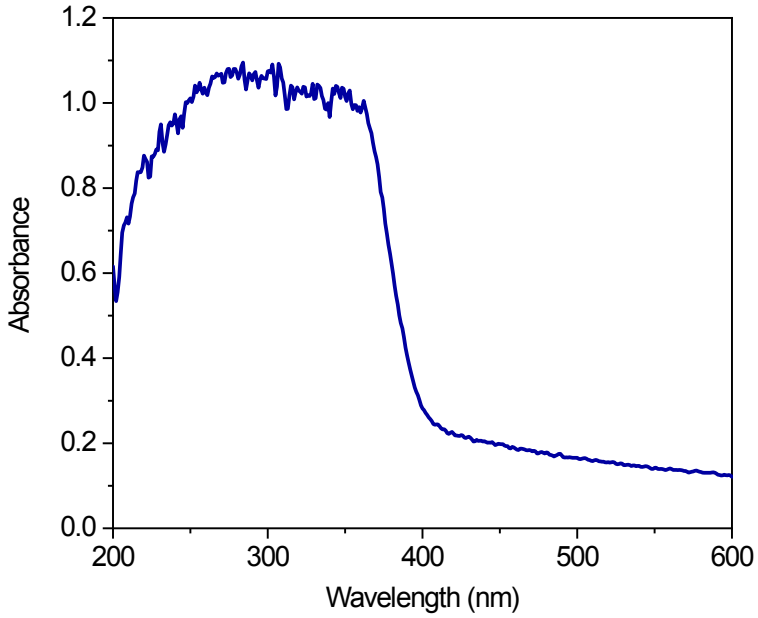

Fig. S9 UV-Visible absorption spectrum of compound **1**.

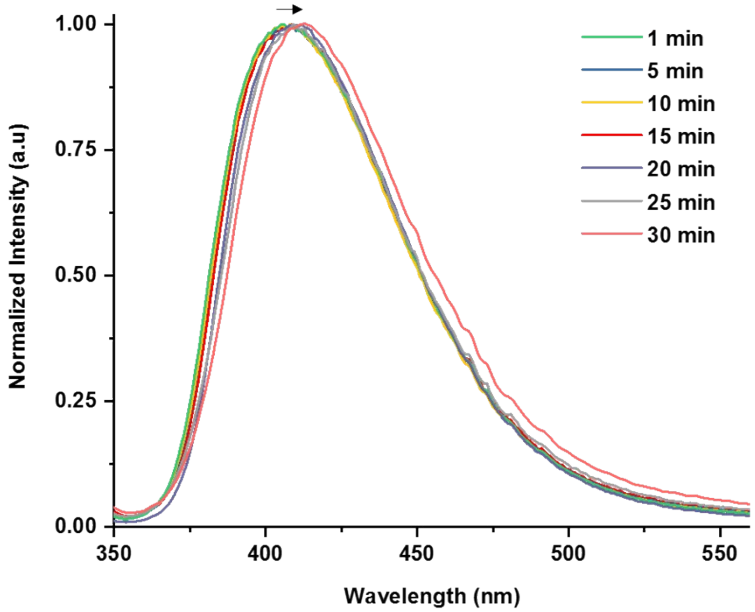

Fig. S10 Solid state photoluminescence spectrum of **1** with different grinding times (Excitation wavelength 330 nm and slit 1 nm). The intensities have been normalized. The PL peak shifts from 406 to 414 nm with increase in grinding time.

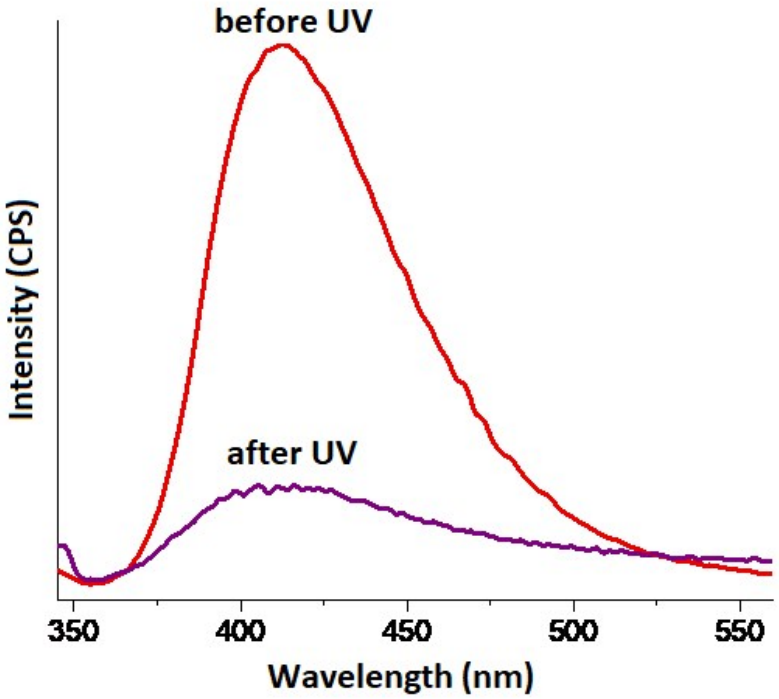

Fig. S11 Solid state photoluminescence spectrum of **1** (30 min ground sample) before and after UV irradiation (Excitation wavelength 330 nm and slit 1 nm). The decrease in the PL intensity is attributed to the loss of π conjugation due to [2+2] photodimerization of 5-Spym ligands.

Density measurement

Experimentally, density measurement was done by following procedure. A known volume of high-density solvent like CCl_4 was taken in a small test-tube and a small amount of ground sample was added to it. Due to lower density of the particles, they floated on the surface of the solvent. Even after shaking the test-tube, most of the particles still stayed on the surface. A low-density solvent like hexane was added dropwise and the test tube was shaken well and let to settle to observe the position and movement of the particles. At a certain point of this procedure, most of the particles remained in the middle of the solvent and showed Brownian motion due to similar density of the solvent mixture and the particles. By taking the mass and volume of the solvent, experimental density of the particles were calculated. In our measurements, as the samples were powder, all the particles did not stay in the middle of the solvent column; some stayed at top and some at bottom forming agglomerates. However, majority of the particles/agglomerates stayed in the middle when the density of the solvent became equal to that of the particles. In order to minimize the experimental error 12-14 measurements were done for each sample and average was calculated.

Isolation of *rctt*-1,3-bis(5′-pyrimidyl)-2,4-bis(phenyl)cyclo-butane (*rctt*-bpcb): The dimerized 5-Spym ligand, (*rctt*-bpcb) was isolated from the complex after dimerization by chemical treatment. The product was treated with conc. HCl to break the complex by precipitating AgCl. After treatment, *rctt*-bpcb was isolated and crystallized in DMSO. The single crystal structure indeed proves that the dimerization occurs in *head-to-tail* manner to form *rctt*-bpcb. Yield (59%). Elemental analysis for **1** (%) Calculated: C 79.09, H 5.53, N 15.37; Found: C 78.88, H 5.37, N 14.16; ^{1}H NMR (400 MHz, 298 K, d_6-DMSO): δ = 8.86 (s, 2H, Pym-H of *rctt*-bpcb), 8.66 (s, 4H, Pym-H of *rctt*-bpcb), 7.25 (m, 4H, Ph-H of of *rctt*-bpcb), 7.21 (m, 4H, Ph-H of *rctt*-bpcb), 7.10 (t, 2H, Ph-H of *rctt*-bpcb), 4.70 (dd, 4H, cyclobutane protons of *rctt*-bpcb).

Crystal data for ***rctt*-bpcb** at 100(2) K (CCDC **1990101**): $C_{24}H_{20}N_4$, M= 364.44; Monoclinic, $P2_1/c$; a = 10.4634(5), b = 8.3919(4), c = 10.5935(6) Å; α = 90, β = 98.999(2), γ = 90°; V = 918.74(8) Å^3; Z = 2; ρ_{calc} = 1.317 g.cm^{-3}; μ = 0.824 mm^{-1}; GOF = 1.051; final R_1 = 0.0505; wR_2 = 0.1336 [for 2267 data $I > 2\sigma(I)$].

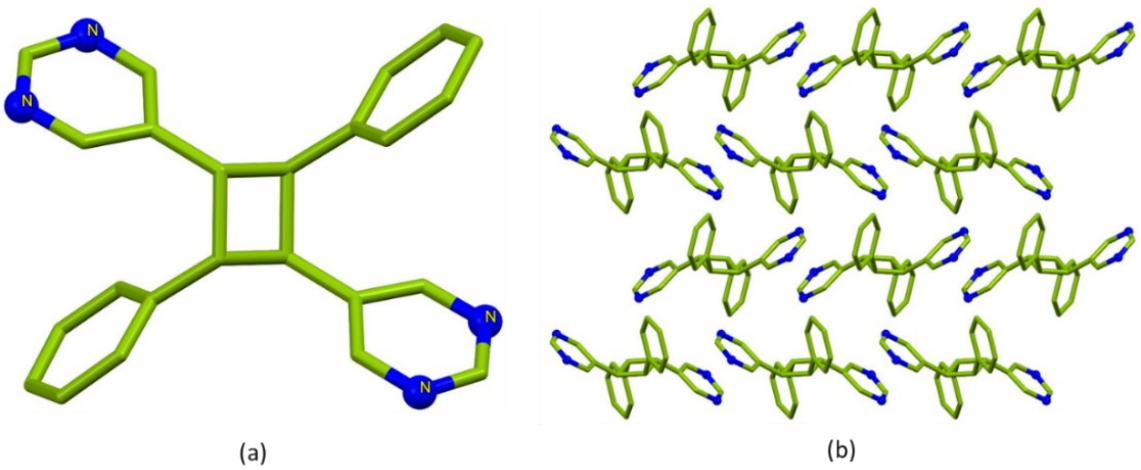

Fig. S12 (a) Single crystal structure of *rctt*-bpcb, confirming the dimerization of 5-Spym in head to tail fashion. (b) Crystal packing of *rctt*-bpcb viewed along *a*-axis.

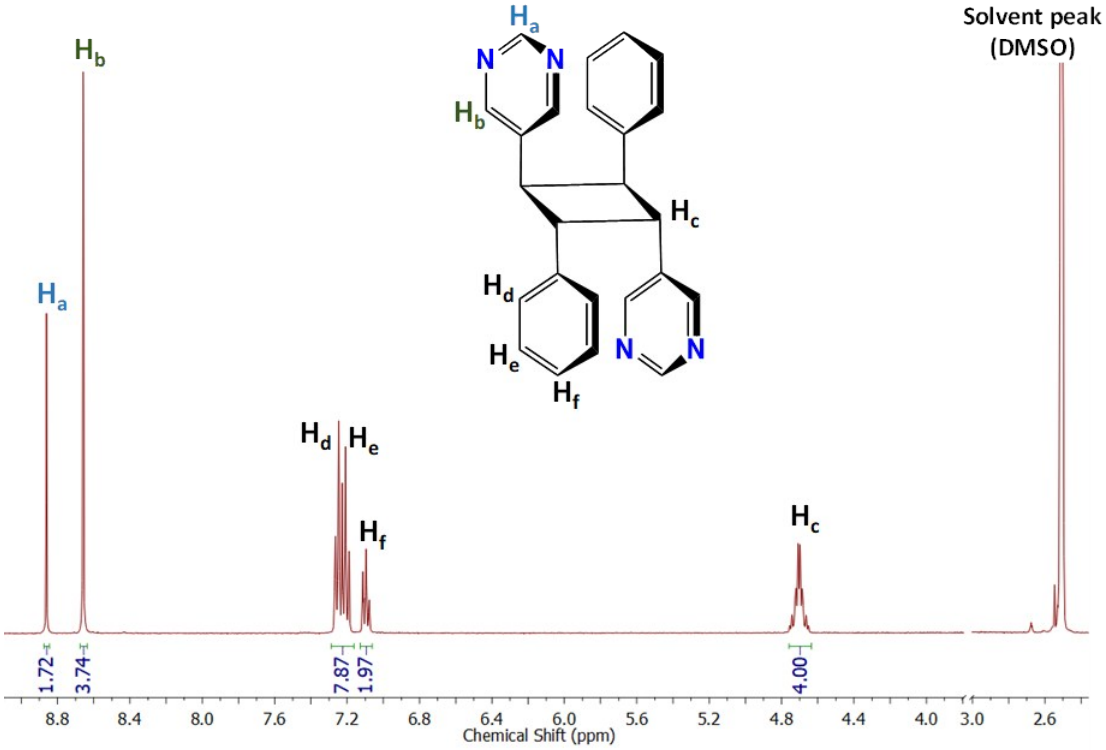

Fig. S13 ^{1}H-NMR spectra of isolated *rctt*-bpcb in DMSO-d_6.

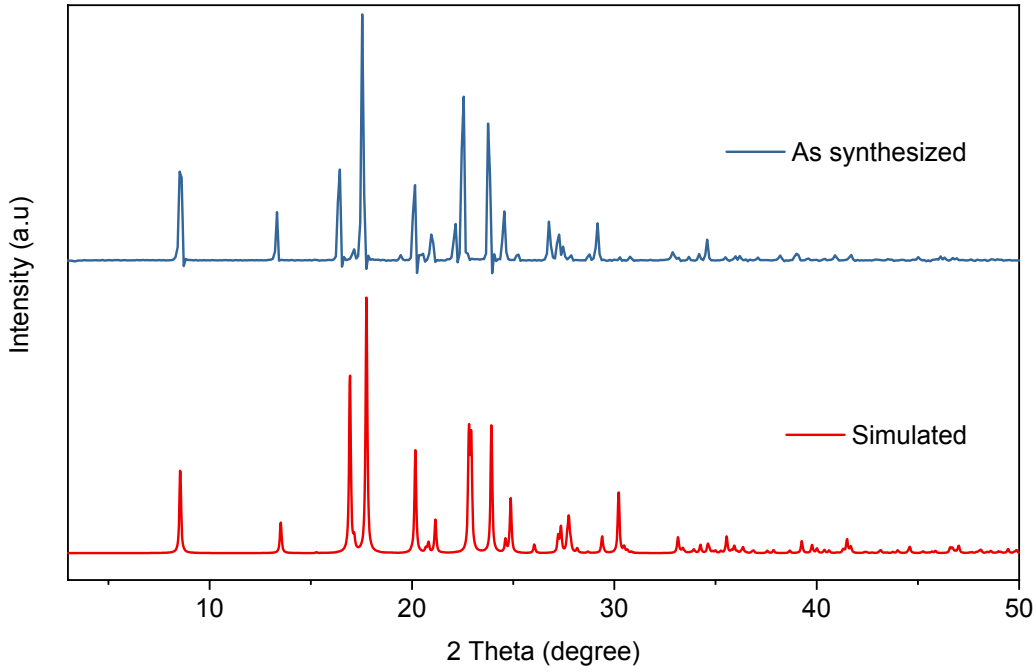

Fig. S14 Comparison of simulated and experimental PXRD patterns of isolated *rctt*-bpcb.

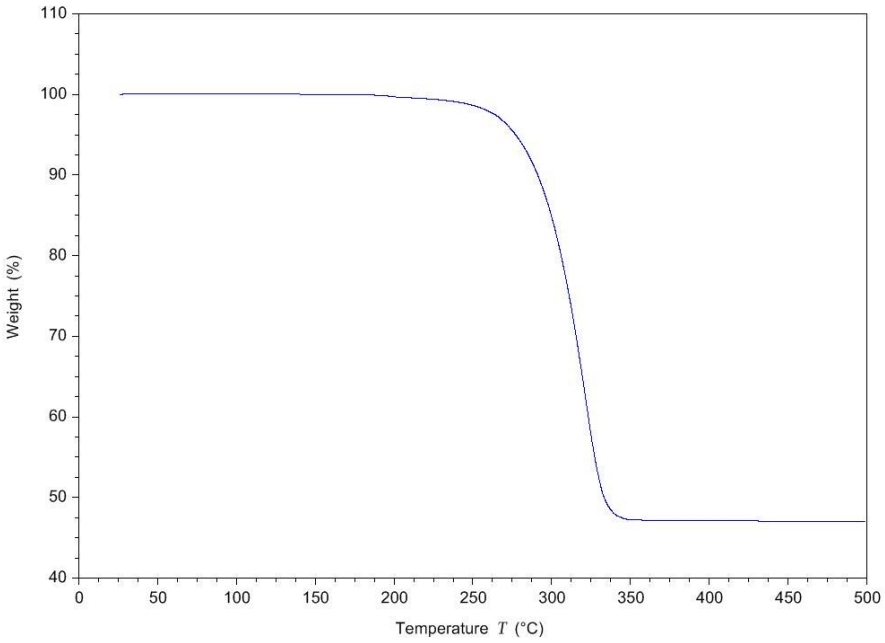

Fig. S15 TGA curve of ***rctt*-bpcb**.

TOPAS measurements

Si powder was mixed with NIST 660a Corundum standard and analysed to obtain instrument broadening profiles, instrumental parameters and exact Si lattice constants. A known weight of Si was then ground with a known weight of MOF compound that had been ball-milled for

a different time. This then gives a known internal standard to allowing all instrument parameters such as zero error and sample displacement to be calculated with certainty.

All data was collected on a PANalytical X-pert Pro using a low background holder. A 1/8" and ¼" slits along with a 0.02rad soller slit were used on the incoming beam, whilst a 0.2 rad soller slit and 5mm receiving slit were used with the detector set in 1D mode with a linear PSD opening of 2.15°. Data was collected twice from 3 – 80 °2θ using a step size of 0.016 °2θ and a time per step of 90s. The sample was spun during collection. The two data sets were added together to improve the peak to background ratio.

All patterns were analysed using TOPAS v6. A typical refinement went as follows: The known instrument parameters were added in along with the known Si STR file and held constant throughout all refinements. The background was calculated using the minimum number Chebyshev order and a 1/x background term when deemed appropriate. The sample height was calculated against the internal Si standard. The unit cell obtained from the single crystal of compound **1** was used for the first 1 minute grinding sample, then the refined unit cell was used as the starting cell for the next grinding time. The Pawley refinements allowed the unit cell parameters to vary, along with a Lorentzian crystallite size parameter.

Table S1

Sample Grind Time	*a* (Å)	*b* (Å)	*c* (Å)	β (°)	*V* (Å³)	Particle Size (LVol-IB) (nm)	Rwp (%)	GOF
1	26.4759(5)	9.1166(1)	28.0833(5)	111.5240(1)	6306.2(2)	87.9(8)	8.21	1.63
5	26.4830(5)	9.1161(2)	28.0900(5)	111.525(1)	6308.6(2)	79.4(8)	9.28	1.54
10	26.5179(6)	9.11383)	28.0879(6)	111.527(2)	6314.7(3)	66.4(6)	8.97	1.49
15	26.5166(7)	9.1143(2)	28.0864(6)	111.516(2)	6315.0(3)	71.2(6)	8.77	1.48
20	26.5310(7)	9.1115(2)	28.0967(6)	111.565(2)	6316.6(3)	50.6(5)	6.97	1.36
25	26.524(2)	9.1096(6)	28.098(5)	111.555(5)	6314.4(8)	36.5(5)	11.06	1.76
30	26.54(1)	9.112(3)	28.096(9)	111.50(3)	6321.8(3.8)	11.5(2)	7.71	1.48

TOPAS refinements become increasingly difficult as the particle size gets smaller and the amorphization increases. Despite these shortcomings, the TOPAS results corroborate with the density measurements, thus render support to the anisotropic volume expansion.

Reference

1. B. B. Rath, G. K. Kole and J. J. Vittal, *Cryst. Growth Des.,* 2018, **18**, 10, 6221–6226.
2. A.A. Coelho, *J. Appl. Crystallogr.,* 2018, **51**, 210–218.